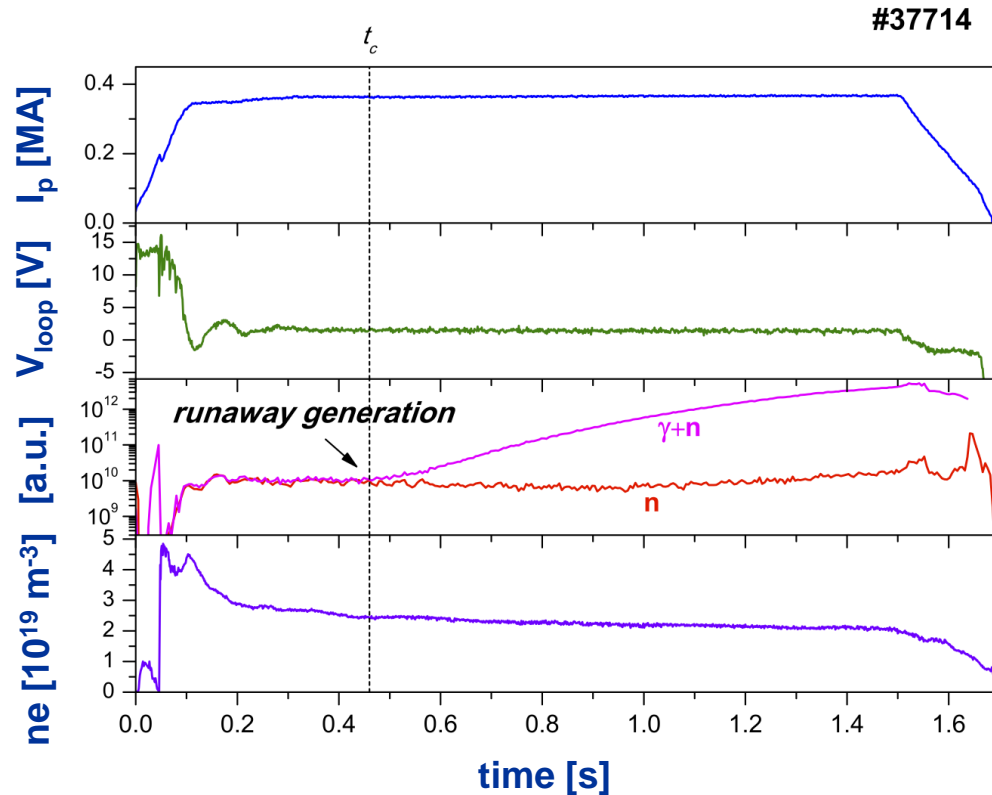


Overview of the FTU results -2015

- ✓ Runaway electrons generation and control
 - Threshold electric field for runaway electron generation
 - Runaway electrons control
- ✓ ECW experiments
 - Real time control of MHD instabilities
 - Amplification of TM by central EC power
 - EC assisted plasma start-up
- ✓ Lithium Limiter experiments
 - Thermal load on the new lithium limiter
 - Elongated plasmas
- ✓ Plasma response to neon injection
 - Peaked density profiles
 - Tearing mode instabilities
- ✓ MHD and SOL studies
 - MHD signals as disruption precursors
 - SOL heat flux width
- ✓ Diagnostics
 - Cherenkov probe
 - Gamma camera
 - Laser Induced Breakdown Spectroscopy

Runaway electrons generation



□ Conditions for RE generation in ohmic pulses investigated for a wide range of toroidal magnetic fields and plasma currents.

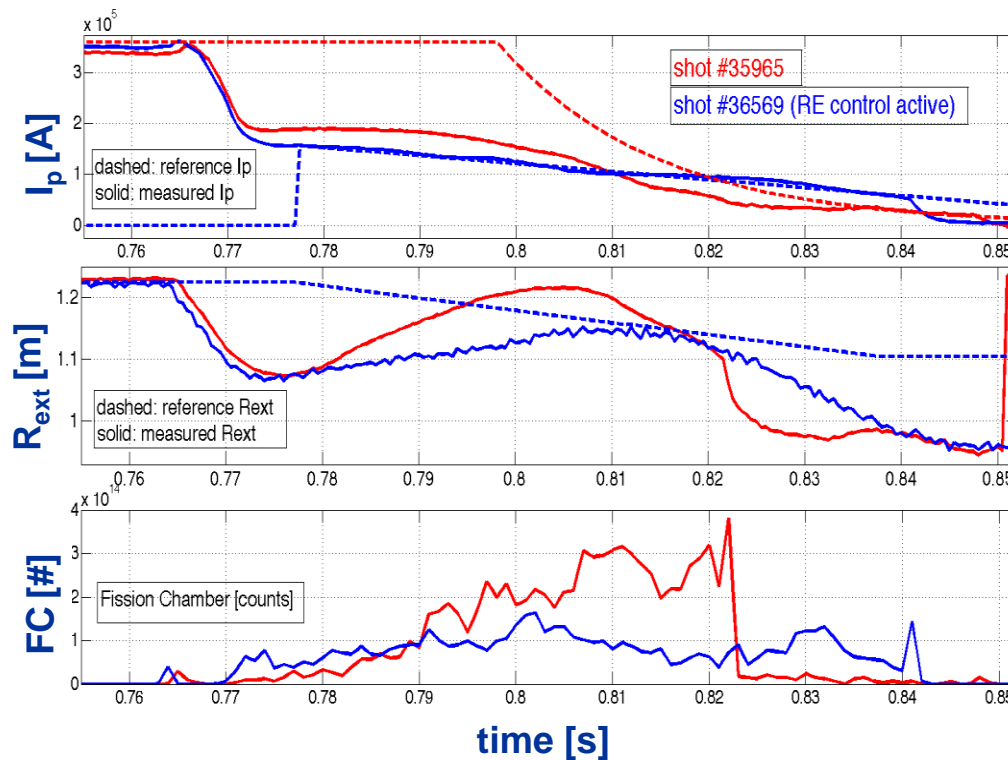
□ Critical electric field for RE generation 2÷5 times larger than the one from collisional theory.

□ Results agree with the new threshold calculated including synchrotron radiation losses.

□ Determination of the threshold density value to be achieved by means of massive gas injection for RE suppression in ITER.

Esposito B. IAEA EX/P2-50 (2014)

Runaway electrons control



□ New RE control algorithm tested for real-time control of disruption-generated RE beam.

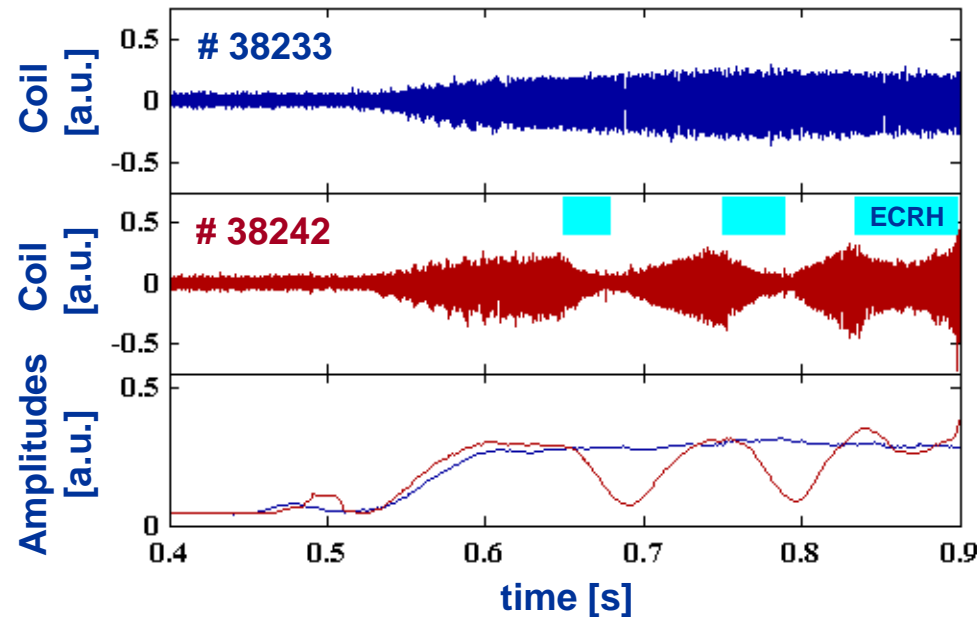
□ Minimize interaction with plasma facing components while RE current is ramped-down by induction.

□ Fission chambers signals show reduced plasma facing components interaction with the new controller.

□ Reduction of the dangerous effects of RE during disruptions in ITER operation.

Carnevale D. IAEA EX/P2-48 (2014)

Real time control of MHD instabilities



Real time control of MHD instabilities using the new EC launcher with fast steering capability (1 deg / 10 ms).

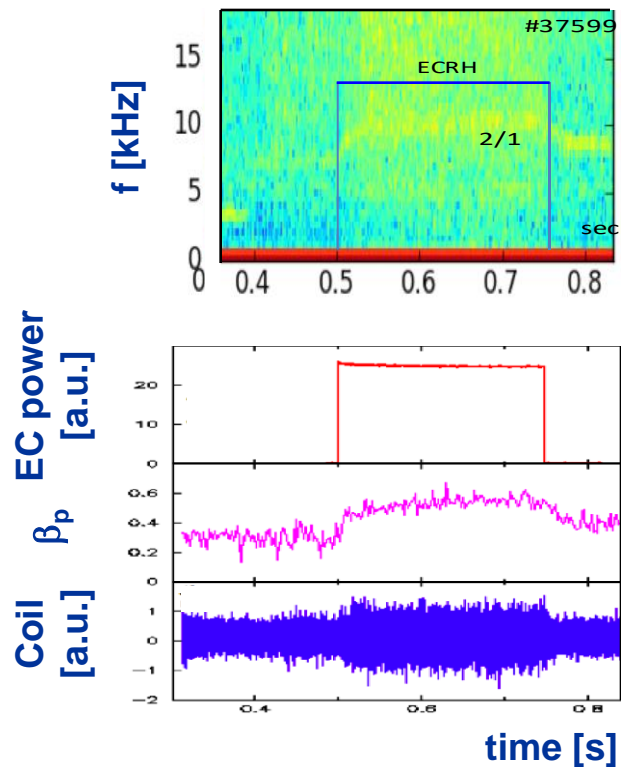
Low-order tearing modes induced by neon injection or by near-limit density.

The data show a marked sensitivity of the resulting instability amplitude to the ECW deposition location.

The experimental condition (control tools essential and based on a minimal set of diagnostics) mimics the situation of a fusion reactor.

Sozzi C. IAEA EX/P2-47 (2014)

Amplification of TM by central EC power



□ Amplification mechanisms by EC due to:

- Modification of the local plasma current density and of the mode stability parameter Δ'_0 .
- Increased bootstrap effect proportional to β_p .

2/1 NTM classification due to the instability amplification by increased bootstrap effect

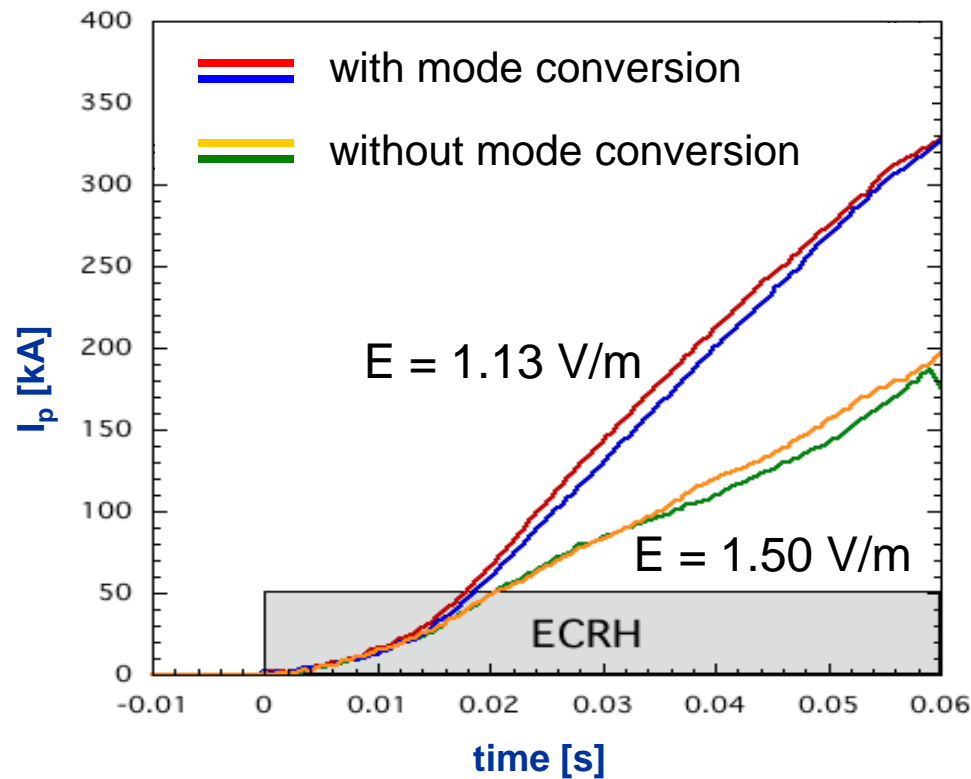
□ Frequency increase due to torque action originated from the applied co-ECCD.

No effect due to modification of rotation (ion polarization effect) because of the amplified size of existing perturbation.

□ Important issue for the fusion plasma operations to avoid the degradation of the plasma confinement due to resistive instabilities.

Nowak S. IAEA EX/P2-54 (2014)

EC assisted plasma start-up

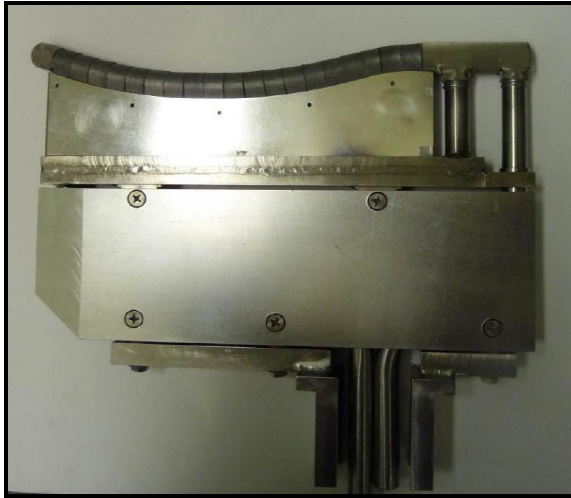


- ▣ Variations of launching angle: OX polarization conversion at reflection from inner wall → better power absorption → higher T_e → lower resistivity.
- ▣ Variations of field null position via external vertical magnetic field.

▣ Experiments focused on ITER start-up issues: start-up at low toroidal electric field (0.5 V/m), even in presence of a large stray magnetic field (10 mT).

Granucci G. IAEA EX/P2-51 (2014)

Thermal load on the new lithium limiter

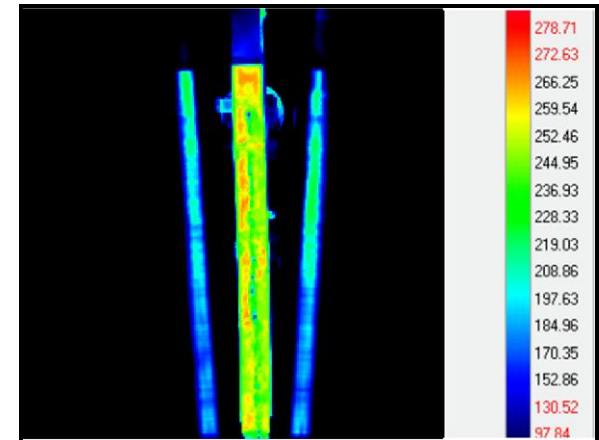


❑ New actively Cooled Lithium Limiter (CLL) with 200°C pressurized (30 bar) water circulation. 10 MW/m² target heat load.

❑ CLL inserted close to the LCMS (2 MW/m²), without any damage to the limiter surface.

❑ Heat load on the CLL from fast IR camera (■ 230°C).

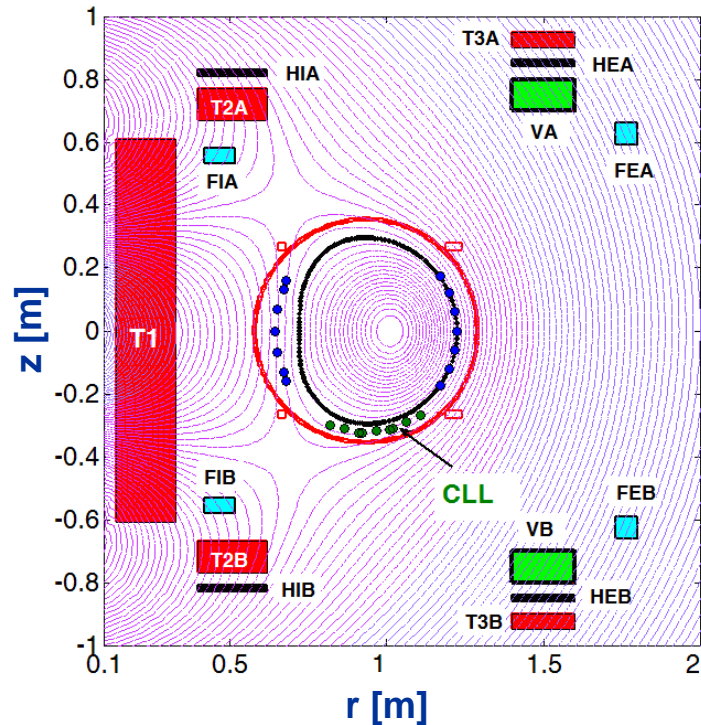
❑ 5 s dedicated pulses in preparation.



❑ Liquid metals could be a viable solution for the problem of the power load on the divertor for steady state operation on the future reactors.

Mazzitelli G. IAEA EX/P2-46 (2014)

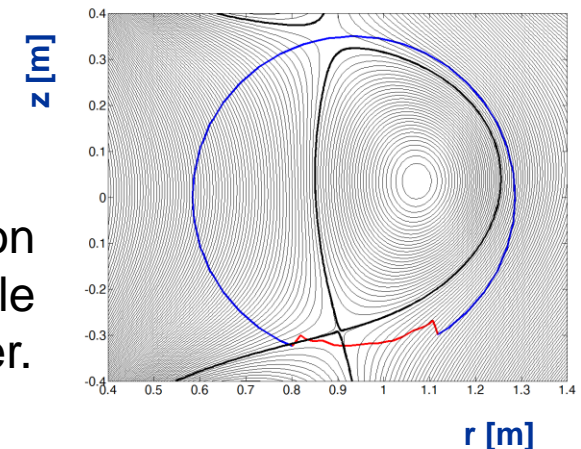
Elongated plasmas



□ Elongated plasmas (5.5 T, 200 kA, $k \sim 1.2$) with ECW additional heating (500 kW).

□ Vary local magnetic shear (flux surfaces opening) at the CLL.

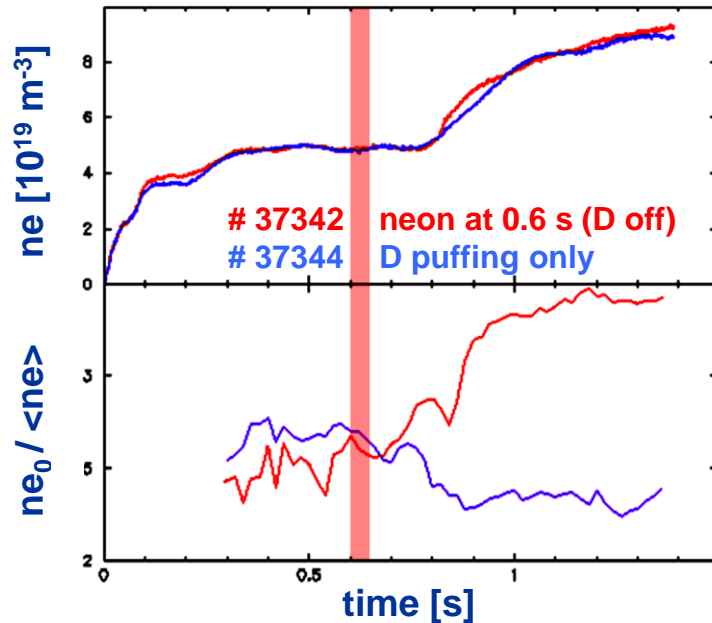
□ Study on-going:
X-point configuration with a magnetic single null inside the chamber.



□ Aim at investigating H-mode access, thus having the possibility to study the impact of ELMs on the CLL used as first limiter.

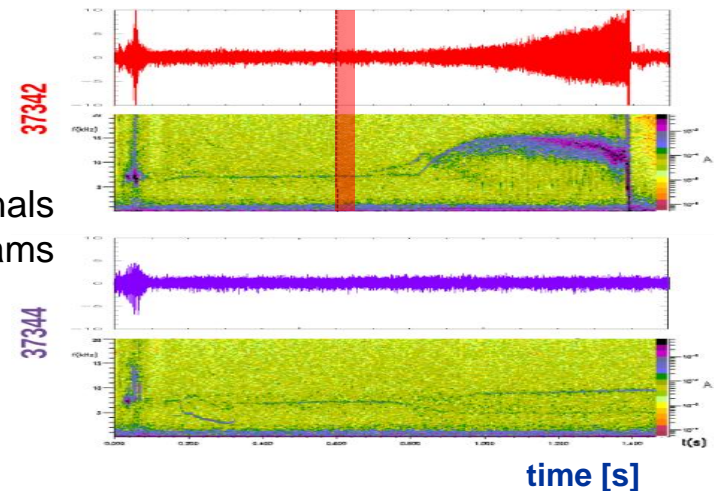
Calabrò G. EPS P4.005 (2014)
Ramogida G. SOFT P2.014 (2014)

Plasma response to neon injection



- ☐ Density peaking increases in response to neon puffing.
- ☐ More inward pinch than in the reference case at the same density without neon puffing.

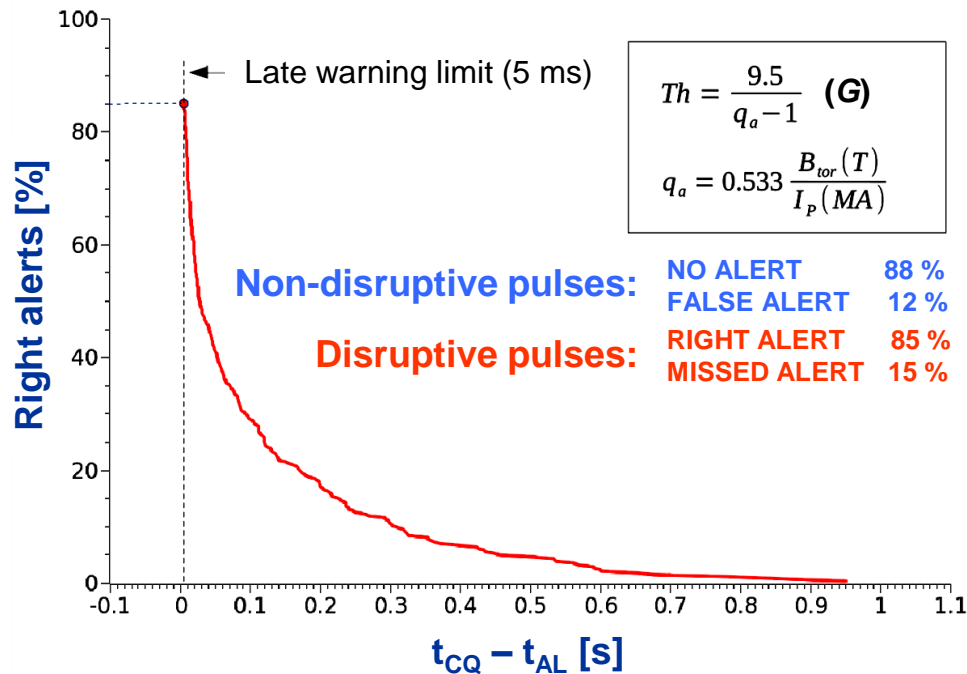
Mirnov coil signals
and Spectrograms



- ☐ Onset or amplification of low-order tearing modes.

☐ It is important to determine the conditions of an increase of particle confinement while minimizing the amount of impurities needed.

Mazzotta C. IAEA EX/P2-52 (2014)
Botrugno A. IAEA EX/P2-53 (2014)



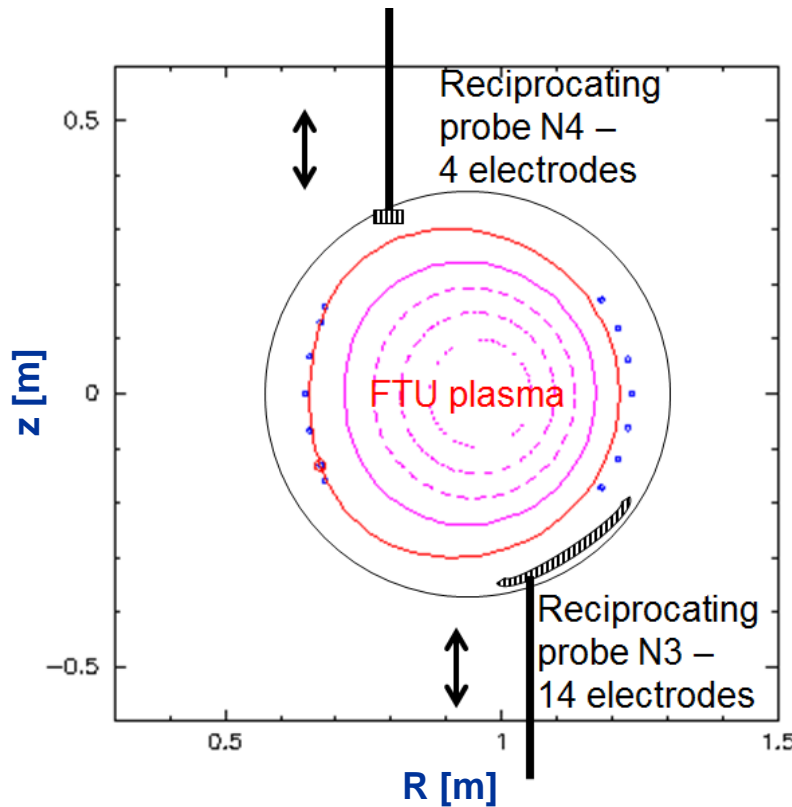
❑ Full real-time algorithm for disruption prediction, based on MHD activity signals from Mirnov coils.

❑ Threshold parameterization in terms of plasma parameters (B_T , I_p) optimized for maximum of timely right alerts and minimum of false alerts.

❑ Threshold optimization on 2000 pulses covering a wide range of physical parameters.

❑ The definition of suitable disruption precursors is of crucial importance in order to trigger actions for avoiding or at least mitigating disruptions.

Cianfarani C. EPS P5.165 (2013)



□ Data collected by two arrays of reciprocating Langmuir probes.

□ Scaling of the heat flux e-folding length λ in the scrape-off layer with:

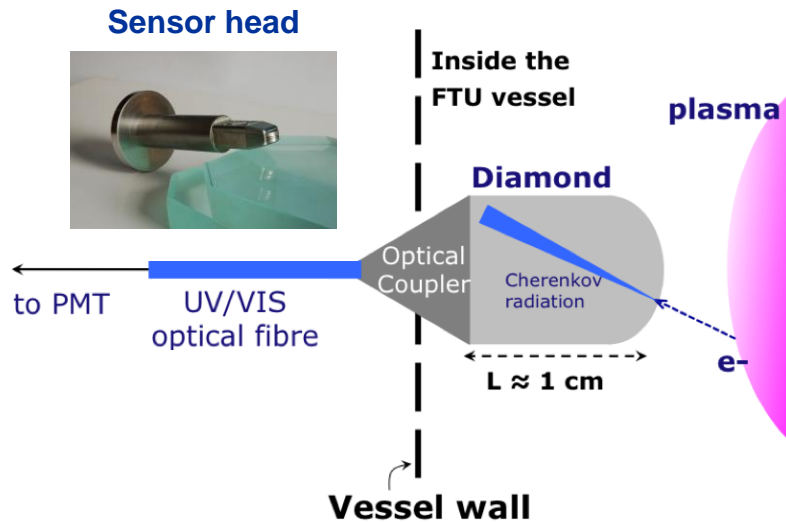
- toroidal magnetic field (B_T)
- plasma current (I_p)
- line-averaged density (n_e)
- power to SOL (P_{SOL})

Strong dependency of λ on I_p ($\sim I_p^{0.6}$) and P_{SOL} ($\sim P_{SOL}^{-0.8}$)

□ This experiment contributed to the multi-tokamak scaling of SOL heat flux width of ITER limiter start-up plasma.

Viola B. EPS P1.119 (2013)

Cherenkov probe

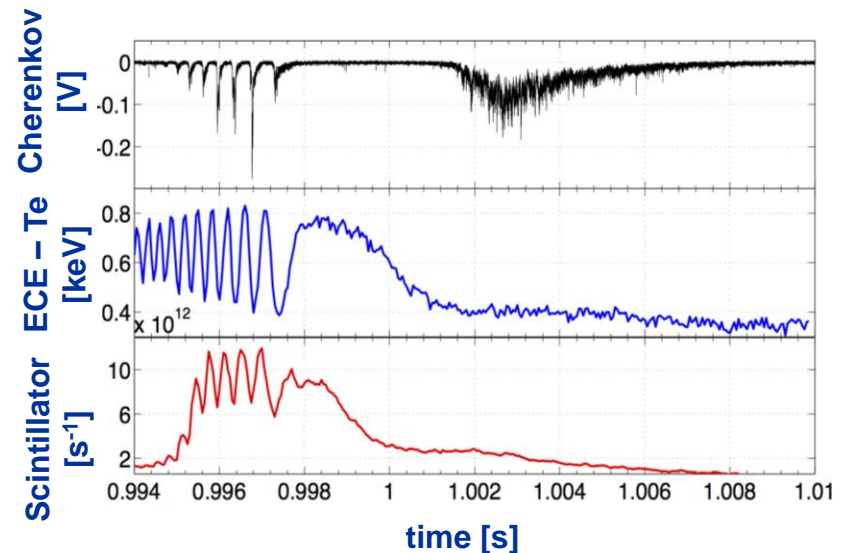


❑ Collaboration with NCBJ.

❑ Escaping fast electrons detected by Cherenkov radiation emitted in diamond probe.

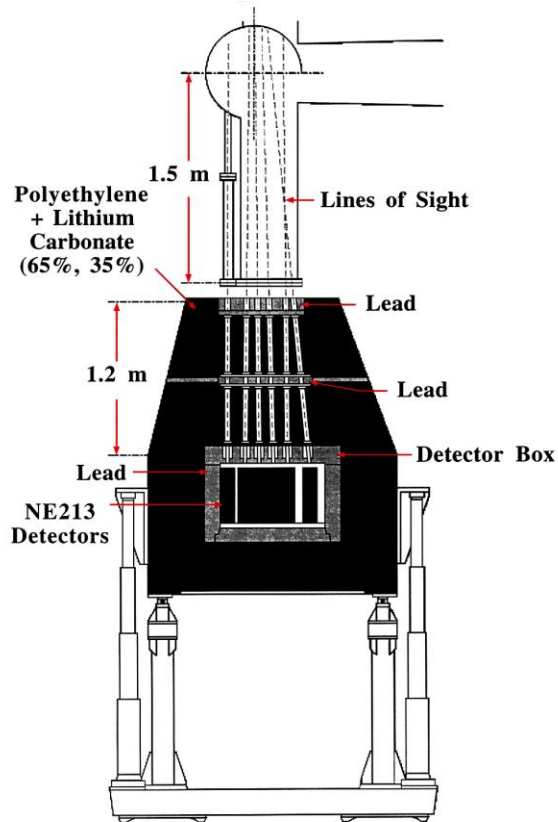
❑ Correlation between Cherenkov signal and magnetic island rotation.

❑ Modelling and simulations (HMGC).



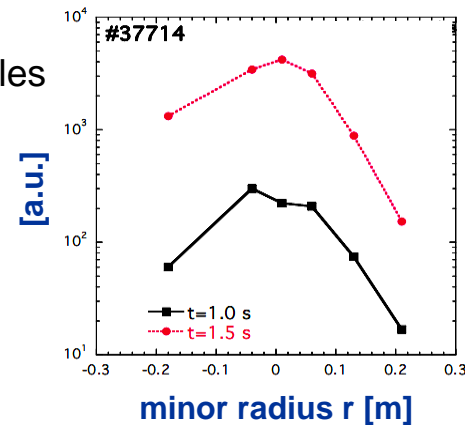
❑ Loss of confinement of fast electrons in the presence of high amplitude magnetic islands.

Causa F. IAEA EX/P2-49 (2014)



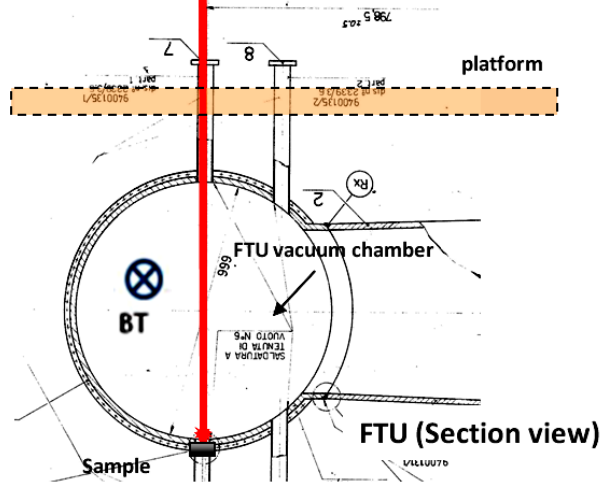
- ❑ Gamma-ray camera for in-flight runaway electrons emission produced by in-plasma bremsstrahlung.
- ❑ Six radial lines of sight equipped with liquid organic scintillators (NE213).
- ❑ n/γ discrimination in conditions of very high count rate.


Hard x-ray profiles



❑ Study of the RE population during the current ramp-up, flat-top and ramp-down phases with sub-ms time resolution.

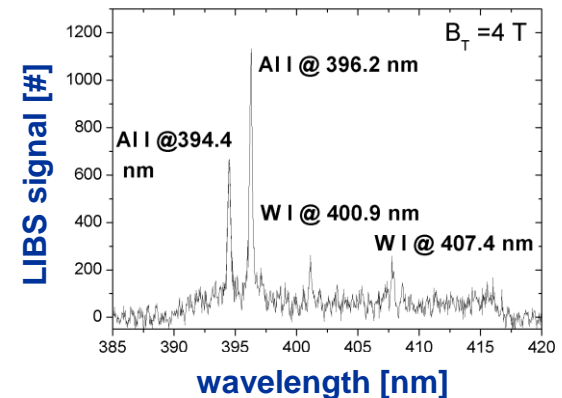
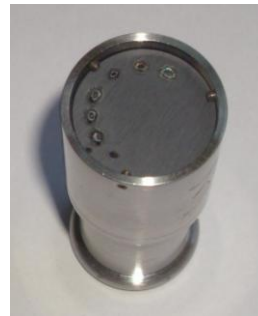
Marocco D. SOFT P2.046 (2014)



 Laser Induced Breakdown Spectroscopy measurements performed on samples placed in FTU vacuum with toroidal field on (up to 4 T).

❑ Experiments demonstrate the feasibility of in situ LIBS diagnostic of surface composition.

Sample W-AI-C



□ Useful information on the surface elemental composition and fuel retention in present and future tokamaks, such as ITER.

Maddaluno G. EPS P5.102 (2013)